PHYSICS LABORATORY

ATUL SINGH ARORA PRASHANSA GUPTA AND VIVEK SAGAR

Advanced Optics Lab

Dr. Mandip Singh
Indian Institue of Science Education and Research, Mohali

January-April, 2013

Atul Singh Arora Prashansa Gupta and Vivek Sagar: *Physics Laboratory,* Advanced Optics Lab,

I have no special talent. I am only passionately curious.
Einstein

ACKNOWLEDGEMENTS

I express my sincere gratitude to our instructor Dr. Mandip Singh for guidance and providing an enjoyable laboratory experience.

I also thank Vivek Sagar (MS11017) and Prashansa Gupta (MS11021) for their valuable contribution to this report as my team members, who made the task of performing experiments immensely comfortable and productive at the same time.

CONTENTS

LIST OF FIGURES

LIST OF TABLES

LISTINGS

ACRONYMS

1 MICHELSON INTERFEROMETER

August 8 and 19, 2012

1.1 AIM

To determine

1. the average wavelength of a monochromatic source
2. the difference in wavelengths of a dichromatic source (Sodium Light)

and to obtain White Light fringes.

1.2 THEORY

The Michelson interferometer demonstrates interference by *division of amplitude* of a wave by partial reflection. The apparatus consists of a source of light, two highly polished plane mirrors, a detector, a beam splitter and a compensating plate. The beam splitter is highly polished at the rear face in order to minimise reflections from the front face. The compensating plate made of the same material and adjusted parallel to beam splitter, essentially makes the path distance travelled in glass by both the beams equal, since one ray undergoes internal reflection while the other undergoes an external reflection; this is important in case the light is not monochromatic (for e.g white light) since refractive index changes with wavelength.

When light from the source falls on the beam splitter, it is partially reflected and partially transmitted in orthogonal directions. These two beams reach the mirrors and are then reflected back into the detector. The fringes can be seen by looking into the mirror through the beam splitter.

Figure 1 [1] explains the formation of fringes. It can be understood by considering replacement of the real mirror M_2 by its virtual image M_2' formed by reflection in G_1. M_2' is parallel to M_1. We may now think of the source as forming two virtual images L_1 and L_2 in M_1 and M_2'. Looking at the mirror M_1, one can see M_1 along with the virtual image M_2' of M_2 formed in G_1. The air film enclosed between M_1 and M_2' is wedge shaped, and we obtain straight line

1 Taken from Jenkins White

fringes. Circular fringes are obtained when the interferometer is in normal adjustment. Depending on the shape of this air film i.e the angle between the mirrors the fringes can be straight, circular, parabolic, elliptical, hyperbolic in shape.

In the given apparatus, both the mirrors can be moved with the help of screws and the distance moved can be measured with a precision of 10^{-7}m. One of the mirrors is mounted on a carriage, whose movement mechanism consists of a large drum. One rotation of this drum moves the mirror by a millimetre. One part of a slow motion smaller drum moves the mirror by 10^{-4}mm. The beam splitter and compensating plate are aligned at 45^{o} to the interferometer arm. The mirrors are provided with two screws at the back which help tilt them so as to adjust them mutually perpendicular.

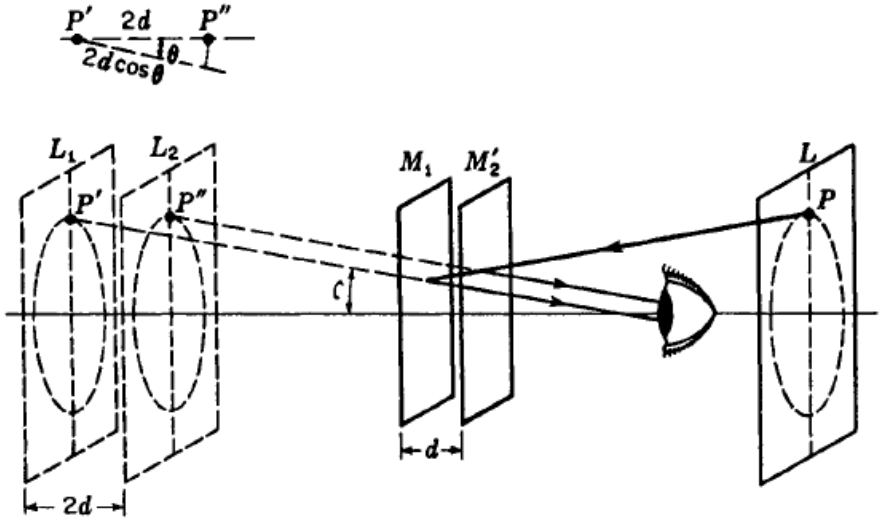

Figure 1: Equivalent Michelson Interferometer Setup

1.2.1 *Determining Wavelength*

The easiest place to begin the analysis of this apparatus would be to ignore the thickness of the beam splitter and the compensator (which is anyway not needed for this experiment) and assume the observations are made at the centre of a far away screen (although in the experiment we've used a lens to focus at infinity). Now at this point, the path difference in the two beams of light would be essentially because of twice the distance between the fixed mirror and the image of the movable mirror. Let this be given by 2d, where d is the distance between the said mirrors. Now imagine a point other than than the centre at the screen. The angle this makes with the principal axis, let

that be θ. The distance light will travel for this point, which can cause phase difference will be $2d\cos\theta$. Keeping in mind the fact that there's an abrupt phase change of π because of reflection at the beam splitter, we have for destructive interference

$$2d\cos\theta = m\lambda \tag{1}$$

and similarly, for constructive interference we'll have

$$2d\cos\theta = (m + 1/2)\lambda \tag{2}$$

It is easy to put in a few numbers [2] and conclude that reducing the distance causes fringes to collapse to the centre (while the spacing between fringes increases). Say for a given configuration, the centre's dark;

$$2d = m\lambda \tag{3}$$

and say for a distance d_o the same is achieved, and N fringes have collapsed to the centre in the process. Then we have

$$2(d + d_o) = (m - N)/\lambda \tag{4}$$

Subtracting these, gives us a simple method of finding the 'average' wavelength of the sodium source

$$\lambda = 2d_o/N \tag{5}$$

1.2.2 *Resolving the D-Lines*

That was the basic theory behind the experiment. Using a little more naiive Math, we can even find the small difference in the Sodium D-lines. Here's how we go about it. First 'd' is made 0. Then the mirror is moved away (or towards) through a distance d. In general, the fringe patterns will overlap in some fashion. Assume a d is such that,

$$2d\cos\theta = m\lambda_1 \qquad 2d\cos\theta = (m + 1/2)\lambda_2 \tag{6}$$

For small θ, we can easily obtain

$$2d/\lambda_1 - 2d/\lambda_2 = 1/2 \tag{7}$$

Observe here what has happened. The maxima of one pattern falls on the minima of the other and vice versa. This means that what we obtain is all bright! Consequently, the pattern disappears in this situation. Making this general, if

$$2d/\lambda_1 - 2d/\lambda_2 = 1/2, 3/2, 5/2.. \tag{8}$$

2 refer to page 15.23 of Ajoy Ghatak, Optics, 4th Edition for details

then the fringe pattern will disappear and for 1, 2, 3 .. it will reappear. Now let us move another step further. ay for an experiment, I find the distance between occurrence of two blank patterns, we have

$$2d_1(1/\lambda_1 - 1/\lambda_2) = 1/2 \tag{9}$$

$$2d_2(1/\lambda_1 - 1/\lambda_2) = 3/2 \tag{10}$$

$$2\Delta d(\Delta\lambda/\lambda^2) = 1 \tag{11}$$

$$\Rightarrow \Delta\lambda = \lambda^2/2\Delta d \tag{12}$$

1.2.3 *Subtle Points*

The theory discussed above is roughly sufficient. Finer points have been posed as questions

1. How does the diffuser help? Can the interference pattern be obtained without the diffuser?
2. What is the wavefront of the waves after they go through a diffuser?
3. Why are the fringes circular? Explain using Huygen's principle (the ray optic method is rather simple).
4. Are the fringes real or virtual?
5. If the light source was in fact a point source, what type of an interference pattern will you obtain? (courtesy sir)
6. In a typical YDSE setup, if we don't use a screen, are we expected to observe fringes?
7. How can we span all angles using just two knobs in the mirror?
8. Can you apply the idea of beats to explain the increase decrease of contrast?
9. What is the expected pattern for a plain wavefront?
10. For a plain wavefront, when a 'dark' pattern is obtained (you'll know once you solve the previous question), where does the energy of the electromagnetic wave disappear? (sir asked this)

1.2.4 *'Practical' Theory*

Some more questions whose answers become clear after playing with the apparatus for sufficiently long

1. What is the primary source of the backlash error in the fine rotation knob?
2. When the average distance of the mirrors from the partly reflecting mirror is higher, why is it harder to get circular fringes?
3. What can cause a uniform rotation of the knob to screw (threaded cylinder) to not cause a corresponding change in the fringe pattern? (basically identify the main cause of this error)

1.3 PROCEDURE

1.3.1 *Obtaining the ring*

It is assumed that you've setup the michelson interferometer in accordance with the diagram in Jenkins White.

1. Move the coarsely moveable mirror to (roughly) the smallest distance from the beam splitter.
2. Now move the other mirror to a slightly larger (you can use smaller also, but then the steps would change correspondingly) distance from the beam splitter, than that of the coarsely movable mirror.
3. Ensure that the pin hole disk is being used.
4. Align the mirror using the three screws provided such that all the four spots coincide (you can choose to look directly without the telescope; in fact that works better usually).
5. Now remove the pin hole disk from the view and put the diffuser (if not already present).
6. Move the moveable mirror at most four times using the coarse movement drum (ensure the movement knob is unlocked) until the fringe pattern is observed. If the pattern is too dense (more than roughly 15 fringes), then follow from the mirror alignment step.
7. Assuming you have roughly 10 fringes at this stage, you now need to bring the centre of the rings into view (if it is already, you're running on beginner's luck).
    a) There are two screws on the mirror and they can roughly be thought of as adjusting the X and Y offset.

b) You'll know you're on the right track if the fringes magnify as you adjust

c) Note that you must leave the knob to know where it really is. Simply holding it also causes the position of the knob to change.

8. If you want further magnification, you can continue rotating and aligning the centre as you go if the need be.

CAVEAT: For certain path differences, the contrast will become very low (as is clear from theory); don't panic.

1.3.2 *Finding* $\lambda_{average}$

Assuming you have obtained the ring already;

1. Set the movement to fine using the lock knob on the apparatus.
2. Place the telescope if you haven't done that already, such that one of the rings is just at the cross-wire.
3. Move the fine rotation knob until the fringes just start to move.
4. Now keep track of the rotations and count 20 fringes as they cross the cross-wire.
5. Repeat this to get sufficient observations

1.3.3 *Finding* $\lambda_{separation}$

Assuming you've obtained the ring;

1. Lock the movement to fine using the lock knob
2. Move the fine rotation until all the fringes disappear and just begin to appear
3. Note the position at this point
4. Now continue rotating the knob until the fringes disappear again and just begin to appear
5. Note this position again
6. Repeat this to get sufficient observations

1.4 OBSERVATIONS AND CONCLUSION

In accordance with Figure 2, the wavelength of sodium light (average) was found to be $620 \pm 65 nm$. Figure 3, the difference in wavelengths was found to be $0.67 \pm 0.15 nm$.

1.5 SOURCES OF ERROR

- The back and forth movement of the mirrors is not precise i.e. the mirrors do not remain parallel to the preceding positions. So the setup might not be normally adjusted and the fringes might not be circular.
- The large drum has a gear arrangement that is aligned to move with the thread of the screw. This calls for a significant amount of backlash error which means that while the screw moves, the fringes don't contributing to erroneous results.
- While noting the positions when the fringes reappear, the contrast of the fringes is noted by the human eye. This contrast almost doesnot vary over almost a rotation of the small screw.

S.No.	Initial reading	Final reading	d = Total width of 20 fringes *10^-7 m
1	42	107	65
2	23	96	73
3	65	117	52
4	20	76	56
5	76	148	72
6	52	120	68
7	20	83	63
8	83	151	68
9	55	108	53
10	8	64	56
11	64	119	55
12	19	90	71
13	30	100	70
14	10	69	59
15	73	130	57
16	60	114	54
17	30	84	54
18	84	139	55
19	94	160	66
20	10	72	62
21	95	158	63
22	58	120	62
23	0	71	71
24	5	65	60
25	58	124	66
		Mean	62.04
		Std. dev	6.569505309

Average wavelength of Na light = 620 nm

Abs. error = 65 nm

Figure 2: Michelson Interferometer: Observations

	D = Distance between the fringes of minimum contrast * 10^-7 m
	2910
	2822
	2835
	2886
	2800
Mean	2850.6
Std dev	40.99560952

Separation between the fringes = 0.67 nm
Rel. error = 2(rel. error in λ) + rel. error in D = 0.232
Abs error = 0.156 nm

Figure 3: Michelson Interferometer: Observations

2 ACOUSTIC DIFFRACTION

August 26 and 27, 2012

2.1 THEORY

Certain assumptions made in the following discussion have been explicitly stated here for clarity.

1. The diffraction grating formed has almost zero thickness
2. A diffraction pattern is observed only when a standing wave is produced
3. Snell's law can be ignored in the consideration of the diffraction pattern

The idea of the experiment is to estimate the speed of sound in distilled water, by producing an acoustic diffraction grating. The setup is as shown in Figure 4.

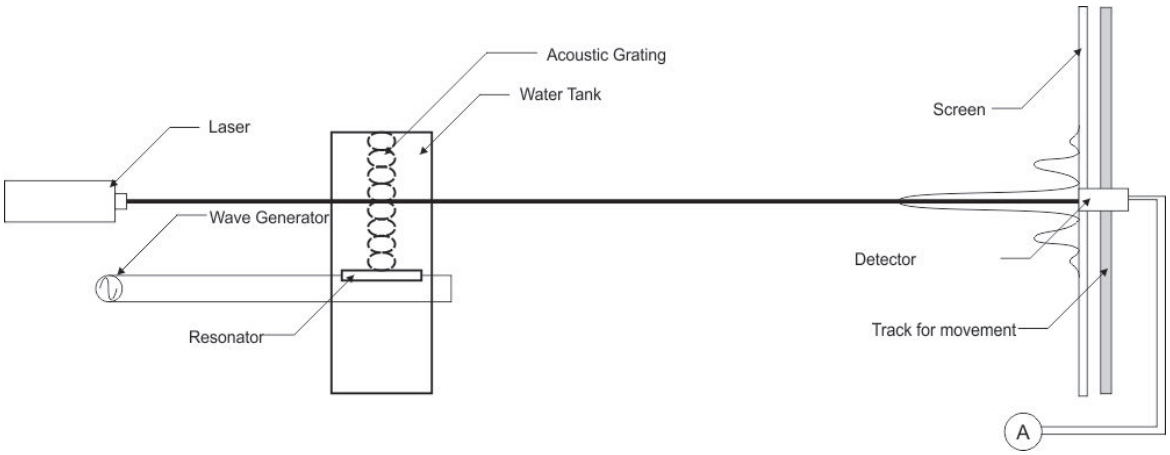

Figure 4: Setup for Acoustic Diffraction

Debye and Sears, in 1932 demonstrated that light diffracts while it passes through a liquid medium excited to ultrasonic vibrations. They explained it by saying that the density maxima and minima of the standing wave obtained in the liquid behaved like an optical diffraction grating, where the grating constant was the wavelength of this ultrasonic wave. Therefore, this method can be used to determine the speed of sound in the medium once we have determined the wavelength of sound by measuring the distance between the ultrasonic source and the diffraction image.

The generation of standing wave in a medium causes changes in density due to pressure nodes and anti-nodes of the sound wave. These density fluctuations in turn cause variations in refractive index which diffracts a beam of light travelling perpendicular to the direction of sound as if it had been diffracted from a diffraction grating of spacing $2d = \lambda_{sound}$ for a standing wave. The sound field is set up by driving a piezoelectric crystal at a given frequency.

The setup consists of a laser, an ultrasonic probe i.e. a piezoelectric crystal, a cuvette filled with a medium (in this case, distilled water), a screen and a frequency generator. The known result $d \sin\theta = n\lambda$ is used for finding d and therefore λ_{sound}, where small angle approximation is used to write

$$0 \sin\theta = \frac{\text{in the plane of the screen, displacement from the centre}}{\text{distance of the grating from the screen}}$$

BRAGG'S DIFFRACTION An electromagnetic radiation which reflects from the surface of a substance has travelled less distance than the one which reflects from a plane of atoms inside the crystal. The penetrating electromagnetic radiation travels down to the internal layer, reflects, and travels back over the same distance before being back at the surface. The distance travelled depends on the separation of the layers and the angle at which the electromagnetic radiation entered the material. For this wave to be in phase with the wave which reflected from the surface it needs to have travelled a whole number of wavelengths while inside the material. Bragg expressed this in an equation now known as Bragg's Law, mathematically stated as

$$n\lambda = 2d \sin\theta$$

where λ is the wavelength of the incident radiation, d is the spacing between the scattering planes and θ the angle between them. It gives the angles at which the radiation, reflected off the scattering plane interferes constructively and produces a peak (a Bragg peak). First proposed by William Lawrence Bragg and William Henry Bragg in 1912, it is used as a tool to study crystals in the form of X-ray and neutron diffraction.

2.2 FURTHER QUESTIONS

- Study braggs diffraction and raman diffraction from Photonics by Teichi
- How does the dimension of the medium affect the pattern?
- Can we realize Braggs diffraction in this experiment?
- Will the diffraction pattern change upon movement of the diffraction grating? Diffraction pattern formation in case no standing waves are formed?

- If the diffraction grating is infinite , will its movement affect the diffraction pattern — it will be phase shifted

2.3 CALCULATIONS AND RESULTS

The observations have been listed in Figure 6. The results have been listed in Figure 7. Figure 5 is the graph obtained.

The speed of sound was found out to be 1312 m/s and 1250 m/s using either sides of the graph.

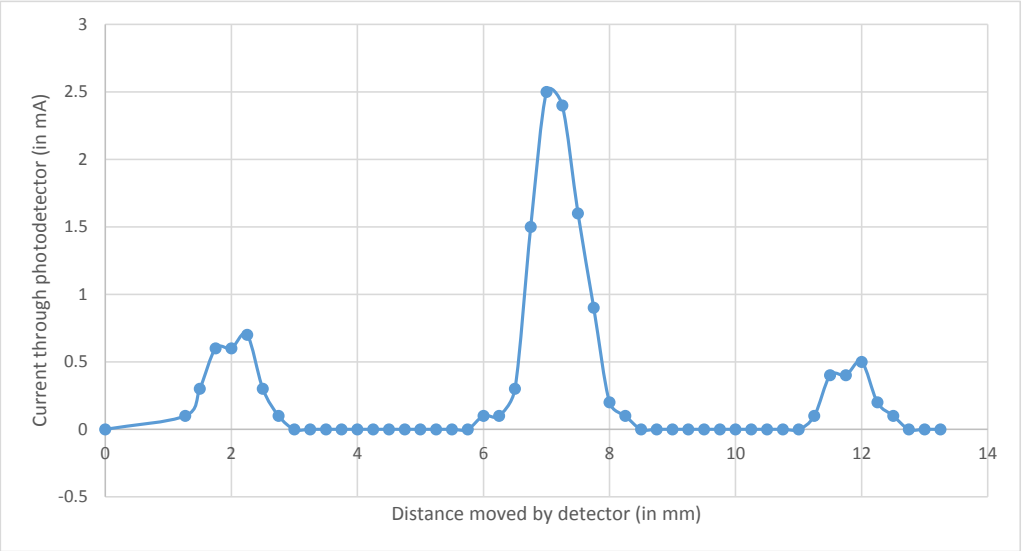

Figure 5: Graph for Acoustic Diffraction

Distance moved by detector (in mm)	Current through photodetector (in mA)
0	0
1.27	0.1
1.5	0.3
1.75	0.6
2	0.6
2.25	0.7
2.5	0.3
2.75	0.1
3	0
3.25	0
3.5	0
3.75	0
4	0
4.25	0
4.5	0
4.75	0
5	0
5.25	0
5.5	0
5.75	0
6	0.1
6.25	0.1
6.5	0.3
6.75	1.5
7	2.5
7.25	2.4
7.5	1.6
7.75	0.9
8	0.2
8.25	0.1
8.5	0
8.75	0
9	0
9.25	0
9.5	0
9.75	0
10	0
10.25	0
10.5	0
10.75	0
11	0
11.25	0.1
11.5	0.4
11.75	0.4
12	0.5
12.25	0.2
12.5	0.1
12.75	0
13	0
13.25	0

Figure 6: Observations for Acoustic Diffraction

Central peak to left peak distance (l1)	4.75 mm
Central peak to right peak distance (l2)	5.00 mm

Distance of detector from grating (D)	1.303 ± 0.005 mm
Wavelength of laser (k)	650 nm
Frequency of RF osc (f)	4.81 MHz
R.I. of water (u)	1.33

Speed of UV sound in water =	2f(Dk)/ul
	1312 m/s using l1
	1250 m/s using l2

Error in measuring l1 and l2 can be crudely estimated by measuring the distance of the points adjacent to the peaks and has been found to be around 10%.

Figure 7: Results and Calculations for Acoustic Diffraction

3

NMR

September 9 to 30, 2013

3.1 T_1, T_2

3.1.1 *Minimal Introductory Theory*

3.1.1.1 *Introduction*

A nucleus of an atom has four intrinsic properties: Mass, electric charge, magnetic moment and the so called, 'spin'. It is important to begin the discussion with the notion of quantization of angular momentum and then reconcile it with the idea of spin. For illustration, consider a rigid diatomic molecule rotating about some axis. This rotating molecule possesses a set of rotational states, in which the total angular momentum L_{tot} has one of the following values:

$$L_{tot} = [J\ (J+1)]^{\frac{1}{2}}\hbar \tag{13}$$

where J takes non negative integer values and $\hbar$ is the reduced Planck's constant. It is worth mentioning that the quantization is a condition on measurement and not a condition on existence. (Basically, (1) gives a discrete set of eigenvalues for the angular momentum operator.) We might ask if there is any state for which (1) doesn't hold; but that will be experimentally unobservable and hence irrelevant. Thus, J completely determines the magnitude of the angular momentum for this system. However, in order to say something about the direction of rotation we need to introduce another quantum number M_J where M_J takes up $2J+1$ integer values from $-J$ to J. In the absence of magnetic field, all these $2J+1$ states are degenerate. However, application of magnetic field breaks this degeneracy. This is called Zeeman effect. The energy separation between the M_J levels is termed as Zeeman splitting.

Spin is also a kind of angular momentum, however, it is not produced due to the rotation of a particle, but is an intrinsic property of a particle, like mass and charge. Matter is built up in such a way that the spins of the different constituent particles cancel out in any large object. Thus, spin is not visible in the macroscopic world. It is precisely because of this reason that the concept of spin is very abstract and unintuitive; it doesn't have a classical analogue.

Spin angular momentum S_{tot}, is given by the following equation:

$$S_{tot} = [S(S+1)]^{\frac{1}{2}}\hbar \tag{14}$$

Here again, S can only take up a discrete set of values. For some particles, S is a non negative integer while for some it is a half integer. The former are called bosons, the latter are named fermions. Thus, an elementary particle like an electron can two kinds of angular momentum; one arising from its motion whilst the other being its intrinsic property. S for an electron is $\frac{1}{2}$.

Now consider a system of two particles. The complete system has a total angular momentum quantum number given by either a sum of two individual angular momentum quantum numbers or their difference or any value in between. For example, consider two particles with spin 2 and $\frac{1}{2}$. The spin quantum number of the system can be $1\frac{1}{2}$, 2 or $2\frac{1}{2}$. Calculating spin for a system of more than two particles is more complicated. For the purpose of this experiment, it suffices to assume that there exists a certain way using which one can describe the spin of the nucleus as a whole. It is reasonable to guess that the total spin of zero corresponds to the state when there is an equal number of nucleons with opposite spin orientations.

3.1.1.2 *Nuclear spin*

Protons and neutrons are made up of quarks. Both are spin $\frac{1}{2}$ particles. Nuclear spin quantum number is denoted by I. Now, consider a proton in a nucleus with a mass number $M > 1$. The other nucleons can have their spin either parallel or anti-parallel to the first proton. Thus, there is a large number of configurations of spins of nucleons possible for a given nucleus. These nuclear states may have an enormous amount of energy difference among them ($\sim 10^{11}$kJ/mol for ^{2}H). There are no simple rules to predict the ground state nuclear spin (the state with the lowest energy), however, a few guidelines are applicable:

1. If the no. of protons and neutrons are both even, the ground state nuclear spin is given by $I = 0$.

2. If the no. of protons and neutrons are both odd, the ground state nuclear spin is given by $I > 0$.

It is worth highlighting that the splitting between the nuclear ground state and the nuclear excited state is an entirely different phenomenon from the Freeman splitting. The former can be ignored in ordinary spectroscopy owing to the huge energy difference while the latter has magnitude far less than the thermal energies.

3.1.1.3 *Microscopic magnetism and spin precession*

Most of the macroscopic objects are observed to display an induced magnetism in the presence of an external field. The induced magnetic moment takes some time to build up. The equilibrium value of the magnetic moment is proportional to the external magnetic field.

$$\mu_{induced} = \mu_0^{-1} V \chi B \tag{15}$$

Where μ_0 is the permeability of the free space, V is the volume of the object and χ is a dimensionless quantity called the magnetic susceptibility expressing how readily the material develops the magnetic moment in the presence of magnetic field. χ can be negative as well, in which case the material is said to be diamagnetic. On the microscopic level, there are three fundamental sources of magnetism in an atom:

1. Circulation of electric current due to orbital motion of the electrons.
2. Magnetic moments of the electrons.
3. Magnetic moments of the nuclei.

From Faraday's law (and Lenz' law), it can be guessed that the circulation of electric current contributes a negative value to the susceptibility, whilst the other two have positive contributions. In paramagnetic substances, i.e. the substances with positive χ, the latter two contributions dominate over the first. A symmetry rule in quantum mechanics dictates that the spin and magnetic moment operator have the following relation:

$$\hat{\mu} = \gamma \hat{S} \tag{16}$$

For a nucleus, γ is called the gyromagnetic ratio, different for different isotopes. Now, consider a macroscopic bar magnet in an external magnetic field B. The magnet has a magnetic moment μ along its axis. In this scenario, the tendency of the bar magnet is to rotate and orient itself in the parallel (or anti-parallel) to the direction of the applied magnetic field. However, (4) gives rise to a whole new phenomenon in case of quantum particles like nuclei. In this case, there is a precession of angular momentum (and thus, magnetic moment) around the direction of applied magnetic field. Thus spin polarization (direction of spin angular momentum) sweeps a cone around the magnetic field, keeping a constant angle between the spin magnetic moment and the field that depends only on the initial spin polarization. The frequency of this precession is proportional to the external magnetic field.

$$\omega^0 = -\gamma B^0 \tag{17}$$

Where ω^0 is called the Larmor frequency. The frequency is considered positive according to the right hand thumb rule convention, where thumb points in the direction of B.

3.1.1.4 *Spin-lattice relaxation*

Spin orientations of nuclei of a typical sample, e.g. H nuclei in water, are uniformly distributed in all the directions, the total magnetic moment being very close to zero. In the presence of a magnetic field, all the nuclei begin executing Larmor precession. However, the atoms which contain these nuclei are undergoing 'collisions' with each other. This thermal motion hence, gives rise to slight fluctuations in the magnetic fields that the nuclei experience. At any given time, the local magnetic field experienced by anyone nuclear spin is slightly different, both in magnitude and direction to its neighbour. These small fluctuating fields due to neighbouring atoms cause a gradual breakdown of constant angle 'cone precession' of the nuclear spins. Over a long period of time, the magnetic moment of each nuclear spin wanders around, moving between different 'precession cones' and eventually sampling the entire range of possible orientations.The time scale of precession motion is a few nanoseconds whilst that of the wandering motion can be as large as a second. The thing to notice is this that since the environment has some temperature, it is slightly more probable that the nuclear spin is driven towards an orientation with higher magnetic energy. This anisotropy of the magnetization distribution in thermal equilibrium means that the entire sample acquires a small net magnetic moment along the field, i.e. a longitudinal magnetic moment. It is found that:

$$\chi_{nuc} = \frac{\mu_0 \hbar^2 \gamma^2 c}{4 k_b T} \tag{18}$$

Where c is the number of protons per unit volume. Assume that the magnetic moment at equilibrium is denoted by M_{eq}^{nuc}. Magnetic moment of the material after time t of application of magnetic field to the sample can be approximated by the following relation:

$$M_z(t) = M_{eq}(1 - e^{\frac{-t}{T_1}}) \tag{19}$$

In the above expression, $T_1$is the time constant called the spin-lattice relaxation time constant which depends on the isotope, viscosity and temperature etc.

3.1.1.5 *Spin-Spin relaxation*

The longitudinal nuclear spin magnetization is too weak to be of any experimental importance. The following technique is employed. Suppose that the spin system is allowed to reach a thermal equilibrium,

on microscopic level which corresponds to a large number of nuclear spin magnets precessing around the magnetic field at the same frequency . Let us choose a rectangular coordinate system such that the applied field is in z-direction. There is no net magnetization in the transverse directions. Suppose now an r.f. pulse is applied to the system such that all the spin orientations are rotated by $\frac{\pi}{2}$ to, say x− directions. Once the pulse is removed, all the nuclei begin to precess around $z-$ axis at an angle of $\frac{\pi}{2}$. The net magnetic moment perpendicular to the field applied is called the transverse magnetization. It should be noted that this transverse magnetization will decay with the passage of time because the spin polarizations will cease to precess in synchrony. The factors responsible for making the precession out of sync are lack of homogeneity in the applied magnetic fields, fluctuations in the field due to thermal motion etc. Macroscopic magnetizations at a time t after the pulse has been applied has the form:

$$\begin{aligned} M_y &= -M_{eq}^{nuc} cos(\omega_0 t) e^{\frac{-t}{T_2}} \\ M_x &= M_{eq}^{nuc} sin(\omega_0 t) e^{\frac{-t}{T_2}} \end{aligned} \tag{20}$$

It should be noted that there is an exponential decay with a time constant T_2. This decay constant is termed as the transverse relaxation time constant. It so happens that this rotating magnetic field produces an electric field according to the Faraday's law. If a wire loop is placed at a suitable location near the changing magnetic field, then the electrons of the wire can be brought into motion. Thus a tiny current is generated which can be detected.

3.1.1.6 *NMR Signal*

The oscillating current in the previous expression is called the *NMR signal* or *free-induction decay*. This NMR signal has the information about the Larmor frequency and the time constants.

3.1.2 *Instrumentation Setup*

On a broad level, an NMR spectrometer extracts information about a given sample in three steps.

1. Allowing the magnetic nuclear spins in the samples to reach thermal equilibrium in a large homogeneous magnetic field.
2. Rotating the nuclear spin polarizations by an r.f. pulse.
3. Detecting and amplifying the weak r.f. signals that is emitted as the spins resume their precession motion in the magnetic field.

This poses certain challenges on the machinery. Firstly, the NMR signal is very weak. Secondly the NMR frequencies must be measured

with extremely high accuracies. Thus there are twin challenges of sensitivity and resolution. The spectrometer has following parts:

3.1.2.1 *Magnet*

In order to avoid inhomogeneous broadening, the spectrometer uses a magnetic field with extremely high homogeneity (1 part in 10^9). The NMR spectrometer in the lab employs the use of superconducting magnets. The magnetic field it can produce is of the magnitude 14.7 T. This corresponds to a Larmor frequency of 600 MHz for a TMS Hydrogen. Maintain the superconducting coils (made up of an alloy of Nb and Sn) at a low temperature requires a constant cooling by a bath of liquid helium. The liquid helium bath is itself insulated by another large reservoir of liquid nitrogen. Through the centre of the large cylindrical can of coolant and the superconducting coils there is a large cavity (insulated from the magnets) called bore. The sample is placed on a probe and kept inside the bore so that it experiences the highest magnetic field. The temperature inside the bore can be brought to the room temperature. There are two additional sets of coils called shims. There are two kinds of them: one wound from superconducting material immersed in the liquid helium bath, called superconducting shims and the other supported on a tube that is inserted into the magnet bore, called the room temperature shims. Shims act as a correction for the inhomogeneity of the magnetic field.

3.1.2.2 *The Transmitter Section*

This is the part of the spectrometer that produces the r.f. irradiation. In our instrument there were four transmitter sections each dedicated to producing r.f. signals at frequencies close to the Larmor frequencies of different isotopes: C^{13}, H, F and D. In general the synthesizer output wave of a transmitter section is given by

$$s_{synth} \sim \cos(\omega_{ref} t + \phi(t)) \tag{21}$$

Here $\phi(t)$ is the r.f. phase while the term t is the time coordinate. In general, this term $\phi(t)$ jumps rapidly between different values, the discontinuous phase jumps being controlled by a timing device called the pulse programmer. In general, we need only a short pulse of r.f. and hence it is important to chop out a 'time-slice' of the r.f. waveform. This is done by the pulse gate. The duration of an r.f. pulse is termed as the pulse width. Finally, a radio frequency amplifier is used to scale up the gated and shifted waveform so as to produce a large amplitude r.f. pulse.

3.1.2.3 *The Duplexer*

The amplified r.f. pulse goes to the probe via duplexer. Another cable emanates from the duplexer which goes to the receiver section. The

role of the device is two fold. It makes sure that the pulse from the transmitter section goes only to the probe and not to the the sensitive receiver section. Secondly, the tiny NMR signal goes only to the receiver and not to the transmitter section. There are multiple ways of doing this but the electronics behind the Duplexer is beyond the scope of this report.

3.1.2.4 *The Probe*

The probe has several functions:

1. Locating the sample in a region of homogeneous magnetic field.
2. Exposing the sample to r.f. waves, detecting the r.f. emissions from the sample.
3. Maintaining the temperature of the sample.
4. Rotating the sample to reduce broadening. (at a frequency of around 10 Hz)
5. Using *cryoprobes* to reduce the temperature of electronic circuits to improvise signal detection.
6. Creating controlled inhomogeneity in magnetic field, often needed in diffusion related and imaging experiments.

3.1.2.5 *The Receiver Section*

The receiver section consists of various sub-parts, the first of which is the signal pre-amplifier, responsible for amplifying the r.f. emission from the sample. Secondly, the quadrature receiver combines the NMR signal, which oscillates at the Larmor frequency ω_{ref}, with the reference signal, oscillating at the frequency ω^0, to generate a new signal that oscillates at the relative Larmor frequency $\Omega = \omega^0 - \omega_{ref}$. This is done because for computer analysis, one needs to convert the incoming waveform into a digital signal. However, the present ADC converters can't handle such a high frequency and the latter needs to be brought down, a job accomplished by the quadrature receiver.

3.1.3 *Theory*

3.1.3.1 *Prerequisites*

For this section, it is recommended that chapters 10, 11 and 12 are read from Levitt. However, only the following concepts (for spin 1/2 particles) are required for a working knowledge of the experiments.

1. Law of motion of a spin particle under a constant magnetic field and the associated rotation matrices and angular momentum operators

2. Concept of a rotating frame and the transformed Hamiltonian
3. Equation of motion for precession in the rotating frame
4. Effect of an RF pulse on the Hamiltonian *
5. Understanding of effect of specific pulses like $(\pi/2)_X$ on the spin particle's state ket
6. Effect of a generalized pulse on the state ket and nutation (a qualitative picture would suffice)
7. Density operator; its need, significance and definition
8. For a spin 1/2 system; the physical significance of the terms of the density operator and order of coherence
9. Derivation of the density operator at thermal equilibrium
10. Density operator in the rotating frame
11. Associated to the density operator, the magnetization vector
12. Effect of an RF (strong) pulse on the density operator (using the definition and item 4) *
13. Effect of specific pulses like $(\pi/2)_X$ and $(\pi)_X$ (coherence excitation and population inversion)
14. Free precession without relaxation
15. Phenomenological understanding of transverse and longitudinal relaxation
16. Measurement of T_1 using population inversion and coherence *
17. Measurement of T_2 using Spin Echo *

The starred concepts have been discussed in some detail in this report. The notation is identical to that used in Levitt and the meaning of the symbols may be implied from the context.

3.1.3.2 *Effect of an RF pulse on the Hamiltonian*

When an RF pulse is applied, the spin particle experiences two magnetic fields, one being the static magnetic field and the other being the oscillating field from the excitation coil. The RF pulse is much weaker than the static magnetic field, but is resonant to the precession frequency of the spin particle. As time goes on, the weak RF field brings about a large change in the spin state.

When an RF pulse of phase ϕ_p along the x-axis of the fixed reference system. The oscillations of the RF pulse oscillating at the spectrometer reference frequency ω_{ref}, can be described as the two components rotating in the opposite frequency viz the resonant component

rotating in the same sense as the nuclear spin precession, while the non-resonant component rotating in the opposite.

Neglecting the non-resonant component, the spin hamiltonian during an RF pulse

$$\hat{H} = \omega^0 \hat{I_z} + \hat{H}_{RF}(t) \tag{22}$$

where

$$\hat{H}_{RF}(t) \approx -\frac{1}{2}\gamma B_{RF} \sin\theta_{RF} \cos(\omega_{ref} t + \phi_p)\hat{I}_x + \sin(\omega_{ref} t + \phi_p)\hat{I}_y \tag{23}$$

Apply the sandwich relation to obtain

$$\hat{H}_{RF}(t) \approx -\frac{1}{2}\gamma B_{RF} \sin\theta_{RF} \hat{R}_z(\Phi_p)\hat{I}_x \hat{R}_z(-\Phi_p) \tag{24}$$

where

$$\Phi_P(t) = \omega_{ref} t + \phi_P \tag{25}$$

In rotating frame, the spin Hamiltonian is given by a

$$\hat{H} = \hat{R}_z(-\Phi)\hat{H}\hat{R}_z(\Phi) - \omega_{ref}\hat{I}_z \tag{26}$$

Applying this, we obtain

$$\hat{H} = -\frac{1}{2}\gamma B_{RF} \sin\theta_{RF} \hat{R}_z(-\Phi + \Phi_p)\hat{I}_x \hat{R}_z(\Phi - \Phi_p) + (\omega^0 - \omega_{ref})\hat{I}_z \tag{27}$$

where

$$\Phi(t) = \omega_{ref} t + \phi_{ref} \tag{28}$$

Finally, upon substitution, we obtain

$$\hat{H} \approx -\frac{1}{2}\gamma B_{RF} \sin\theta_{RF} \hat{R}_z(-\phi_{ref} + \phi_p)\hat{I}_x \hat{R}_z(\phi_{ref} - \phi_p) + \Omega^0 \hat{I}_z \tag{29}$$

where Ω^0 is the resonance offset. As is visible, there is no time dependence in the expression.

We can also substitute for ϕ_{ref}, for positive spins it equals π,

$$\hat{H} \approx \omega_{nut} \hat{R}_z(\phi_p)\hat{I}_x \hat{R}_z(-\phi_p) + \Omega^0 \hat{I}_z \tag{30}$$

where the nutation frequency w_{nut} is given by,

$$\omega_{nut} = \|\frac{1}{2}\gamma B_{RF} \sin\theta_{RF}\| \tag{31}$$

Applying the sandwich relation again,

$$\hat{H} \approx \Omega^0 I_z + \omega_{nut}(\hat{I}_x \cos\phi_p + I_y \sin\phi_p) \tag{32}$$

3.1.3.3 *Phenomenological understanding of transverse and longitudinal relaxation*

We know the thermodynamically stable populations of a given spin $\frac{1}{2}$ ensemble. If this population distribution is disturbed, then the system is restored to the equilibrium distribution eventually. This effect is known as longitudinal relaxation, and T_1 quantifies this behaviour.

Similarly, at equilibrium, the coherence is zero. If coherence is introduced, it gradually dies out. This is the transverse relation which is quantified by T_2.

For T_1, we have the following phenomenological equations.

$$\rho_{\alpha 3} = (\rho_{\alpha 2} - \rho_{\alpha}^{eq})e^{-\tau/T_1} + \rho_{\alpha}^{eq} \tag{33}$$

$$\rho_{\beta 3} = (\rho_{\beta 2} - \rho_{\beta}^{eq})e^{-\tau/T_1} + \rho_{\beta}^{eq} \tag{34}$$

$$\text{where } \rho_{\alpha}^{eq} = \frac{1}{2} + \frac{1}{4}\mathbb{B} \tag{35}$$

$$\rho_{\beta}^{eq} = \frac{1}{2} - \frac{1}{4}\mathbb{B} \tag{36}$$

T_1 is typically in the range 100ms - 100s.

For T_2, we have the following equations that describe the phenomenon.

$$\rho_{-3} = \rho_{-2}e^{(i\omega^0 - \lambda)\tau} \tag{37}$$

$$\rho_{+3} = \rho_{+2}e^{(-i\omega^0 - \lambda)\tau} \tag{38}$$

$$\text{where } \lambda = T_2^{-1} \tag{39}$$

We performed an experiment to find λ, as will be discussed in the next sections.

The precise mechanisms of this process has not been dealt with here and only a phenomenological explanation is provided. However, physically one can think of it as follows. On an average the magnetic field (say along $\hat{z}$ is constant) is constant and at an instant t_0 the spins are synchronised. However, there always exist some local fluctuations due to the environment of each individual spin which leads to loss of synchronization, and consequently coherence.

3.1.3.4 *Measurement of T_1 using population inversion and coherence*

Consider the pulse sequence $\pi_X \ \tau \ \pi/2_X$ which is repeated for different values of τ on a given sample and the data is collected for a fixed t. The resulting NMR data can be represented using a 2D data matrix $= S(\tau, t)$. Before proceeding further, some subtleties have been listed

1. In the actual experiment, the acquisition is repeated to reduce errors
2. Each acquisition is separated by time τ_{wait} to allow the sample to return to thermal equilibrium. (τ_{wait} and τ should be much greater than T_1)

3. Something known as a phase cycle is also performed, but has been ignored here (as was done in Levitt, in this discussion)

Let us now look at what the pulse sequence is really doing and then we'll come to the NMR data and its rudimentary analysis. The action of the pulses on the density operator has been re-written for reference.

- π_X generates an inverted population distribution
- $\pi/2_X$ converts the population difference into coherence, including the observable (-1)-quantum coherence.

In terms of the density operator, we can represent the action of the pulse sequence as

$$\hat{\rho}_1 = \hat{\rho}_{eq} = \frac{1}{2}\hat{1} + \frac{1}{2}\mathbb{B}\hat{I}_z \tag{40}$$

$$\hat{\rho}_2 = R_x(\pi)\hat{\rho}_1 R_x(-\pi) \tag{41}$$

$$= \frac{1}{2}\hat{1} - \frac{1}{2}\mathbb{B}\hat{I}_z \tag{42}$$

$$\hat{\rho}_3 = \frac{1}{2}\hat{1} + \frac{1}{2}\mathbb{B}(1 - 2e^{-\tau/T_1})\hat{I}_z \tag{43}$$

$$\hat{\rho}_4 = R_x(\pi/2)\hat{\rho}_3 R_x(-\pi/2) \tag{44}$$

$$= \frac{1}{2}\hat{1} - \frac{1}{2}\mathbb{B}(1 - 2e^{-\tau/T_1})\hat{I}_y \tag{45}$$

The NMR signal then becomes

$$S(\tau, t) = a(\tau)e^{(i\omega^0 - \lambda)t} \tag{46}$$

$$\text{where } a(\tau) = \frac{1}{2}\mathbb{B}(1 - 2e^{-\tau/T_1}) \tag{47}$$

If we plot $a(\tau)$ vs τ, we expect the graph to start with a negative Y intercept, and monotonically rising and then asymptotically stabilizing at $y = \frac{1}{2}\mathbb{B}$.

3.1.3.5 *Measurement of T_2 using Spin Echo*

T_2 as was described physically earlier, arises from the de synchronization of spins which leads to loss of coherence. We therefore first investigate the concept of peak broadening which is essential to understand the need of spin echo in the first place.

Peak broadening is caused primarily be two factors which are called

1. Homogeneous: This arises due to microscopic magnetic fluctuations (quantified by T_2).
2. Inhomogeneous: This is caused by the strong 'macroscopic' magnetic field's inhomogeneity (which is with great pain, attempted to be as homogeneous as possible)

If there were no inhomogeneous broadening, we could easily measure T_2 from the peak broadening. However, there still is a way known as spin echo that can cleverly, selectively measure homogeneous decay, allowing for the measurement of T_2.

Let us look understand inhomogeneous broadening in a little more depth. Figure 12.6 (from Livett) illustrates how multiple spins, when slightly out of phase, cancel out the effect spin, resulting in a sharper decline, and thus a larger peak width.

In the frequency domain, there are many peaks centred around the the peak, which cause the broadening.

We are now ready to discuss the spin echo pulse sequence, the heart of the experiment. The pulse sequence used is $\pi/2_X\ \tau/2\ \pi_Y\ \tau/2$ as is given in figure 12.7 of the text. Let's start as usual with the thermal equilibrium state.

$$\rho_1 = \rho^{eq} = \frac{1}{2}\hat{\mathbf{1}} + \frac{1}{2}\mathbb{B}\hat{\mathbf{I}}_z \tag{48}$$

$$\rho_2 = \frac{1}{2}\hat{\mathbf{1}} - \frac{1}{2}\mathbb{B}\hat{\mathbf{I}}_y \tag{49}$$

From this point onwards, no other pulse converts the populations to coherences, thus the $\hat{\mathbf{1}}$ term will be dropped (as it doesn't contribute to the NMR signal).

$$\rho_3 = \frac{1}{2}\mathbb{B}(-\hat{\mathbf{I}}_y \cos(\omega^0 \frac{1}{2}\tau) + \hat{\mathbf{I}}_x \sin(\omega^0 \frac{1}{2}\tau)e^{-\lambda\frac{1}{2}\tau} + ... \tag{50}$$

$$\rho_4 = \frac{1}{2}\mathbb{B}(-\hat{\mathbf{I}}_y \cos(\omega^0 \frac{1}{2}\tau) - \hat{\mathbf{I}}_x \sin(\omega^0 \frac{1}{2}\tau)e^{-\lambda\frac{1}{2}\tau} + ... \tag{51}$$

$$\rho_5 = -\frac{1}{2}\mathbb{B}\hat{\mathbf{I}}_y e^{-\lambda\tau} \tag{52}$$

And from the last step, we know the peak amplitude in the NMR spectrum will be

$$a(\tau) = \frac{1}{2}\mathbb{B}e^{-\lambda\tau} \tag{53}$$

Do you see the brilliance of the result? Note that the final density operator is independent of ω^0! Which means that the signal is independent of the (inhomogeneity) applied magnetic field and we have successfully found a way of determining λ.

However, we can gain more insight into this mechanism by geometric considerations; by just staring at figure 12.14 - 12.16.

3.1.4 *Practical Implementation*

1. Loading the sample
    a) Ejected the existing item on the air cushion
    b) Loaded the sample using the stairs

2. NMR operation using TopSpin
   Following is a summary of the commands executed to obtain the data. The pulse sequences were changed in accordance with the experiment (T_1 T_2). We were assisted by a PhD student at the NMR lab, with the performance of the experiment.
   a) check no acquisition running
   b) `ebc`: experiment number, title, check solvent used(we use acetone with D), lock field
   c) `rsh`: command for shimming which is done artificially using standard samples by making fields homogenous with respect to them and using them as reference.
   d) `getprosol`: command for retreiving the values of parameters like pulse, duration, delays, aquisition time etc.
   e) `lock`: command to select solvent, we used AcetoneD6
   f) `atma`: automatic tuning matching automatically
   g) `atmm`: automatic tuning matching manually
   h) `rga`: receiver gain automatic
   i) `rgm`: reciever gain manual
   j) `zg`: sets the pulse program t1ir1D, with D1=20s
   k) `starts acquiring FID`:
   l) `efp` : command to perform experimental fourier transformation
   m) `apk`: automatic phase correction
   n) `abs`: automatic baseline correction, it can be done manually too using the command 'absm'

3.1.5 *Observations*

Upon analysis of the existing experimental data, T_1 was found to be $7.43 \pm 0.060(0.81\%)$ for the first and $7.92 \pm 0.059(0.74\%)$ seconds for the second peak, with the corresponding graphs, Figure 8 and Figure 9 and data, 3.1.5. We further found T_2 to be $78.055 \pm 5.739(7.35\%)$ for the first and $84.762 \pm 5.613(6.22\%)$ seconds for the second peak. The corresponding graphs are given in Figure 10 and Figure 11 with the corresponding data in 3.1.5.

It is surprising however that we obtained $T_2 > T_1$ while the theoretic limit is $2T_1 > T_2$, which lead us to the implication that the data we analysed was for two different compounds.

The data corresponding to our experiment was lost before it could be recovered from the NMR machine.

```
D7      Peak 2  Peak 1
0       -0.9949 -1.003
```

```
0.2     -0.9846 -1.0488
0.4     -0.9777 -0.9872
0.6     -0.9004 -0.8968
0.8     -0.8631 -0.8452
1       -0.8028 -0.8031
1.2     -0.7569 -0.7365
1.4     -0.7121 -0.6982
1.6     -0.6718 -0.6574
1.8     -0.6211 -0.6055
2       -0.5692 -0.5698
2.2     -0.5427 -0.5172
2.4     -0.5038 -0.4813
2.6     -0.463  -0.4373
2.8     -0.4205 -0.3974
3       -0.391  -0.3584
3.4     -0.3247 -0.2987
0       -0.9794 -0.99
3.8     -0.2489 -0.2104
4       -0.2162 -0.1791
4.2     -0.1854 -0.1397
4.4     -0.1532 -0.1103
4.6     -0.1229 -0.0819
4.8     -0.0887 -0.0467
5       -0.0637 -0.0231
5.5     0.002   0.0494
6       0.0644  0.1234
7       0.2053  0.2559
8       0.2958  0.3479
```

```
L4      Peak 2  Peak 1
0.2     0.9921  1
1       0.8541  0.9947
10      0.8674  0.95
20      0.797   0.8583
30      0.6809  0.762
40      0.4647  0.5145
50      0.4851  0.5467
60      0.3192  0.3594
80      0.347   0.2621
70      0.2422  0.2853
90      0.2499  0.241
100     0.2331  0.2219
110     0.2209  0.1975
120     0.1963  0.1781
130     0.2062  0.1715
140     0.1864  0.1683
150     0.1933  0.1582
160     0.1939  0.1547
170     0.1621  0.1563
180     0.1636  0.1541
190     0.156   0.1645
200     0.1521  0.162
```

```
210     0.1442  0.1597
220     0.1352  0.1633
230     0.1308  0.1573
270     0.0935  0.1448
250     0.111   0.1502
260     0.1024  0.1465
270     0.0923  0.1398
280     0.0834  0.1329
```

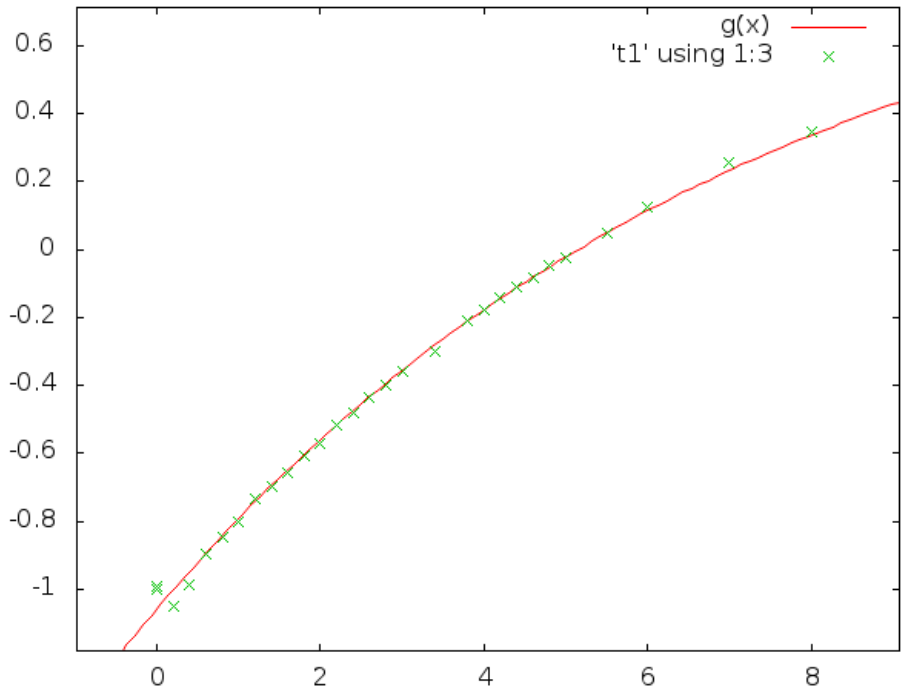

Figure 8: Intensity vs Time (sec), for T_1, peak 1

3.2 DIFFUSION

3.2.1 *Theory*

Cation

3.2.2 *Practical Implementation*

Cation

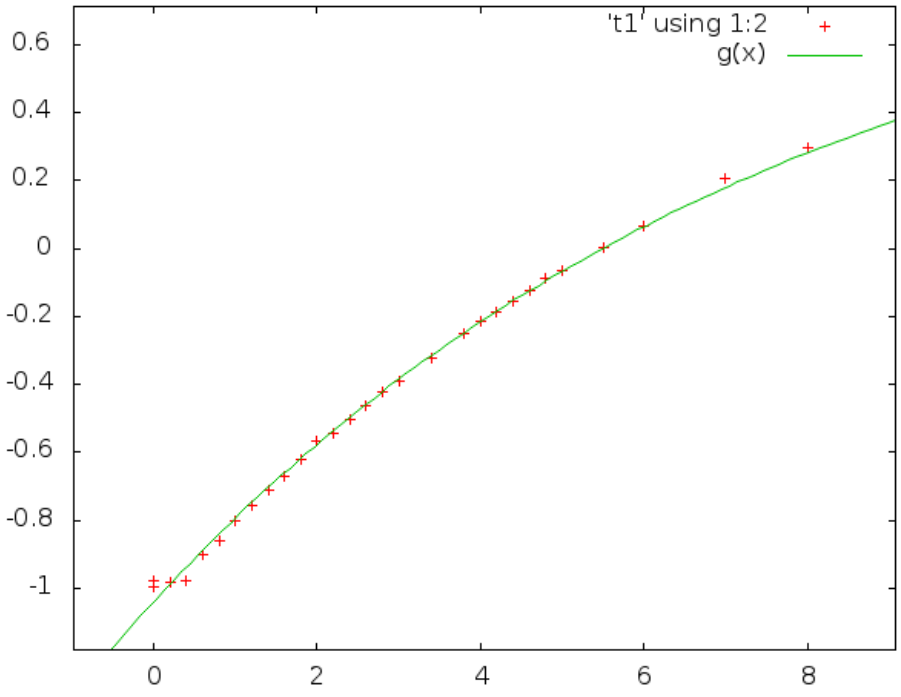

Figure 9: Intensity vs Time (sec), for T_1, peak 2

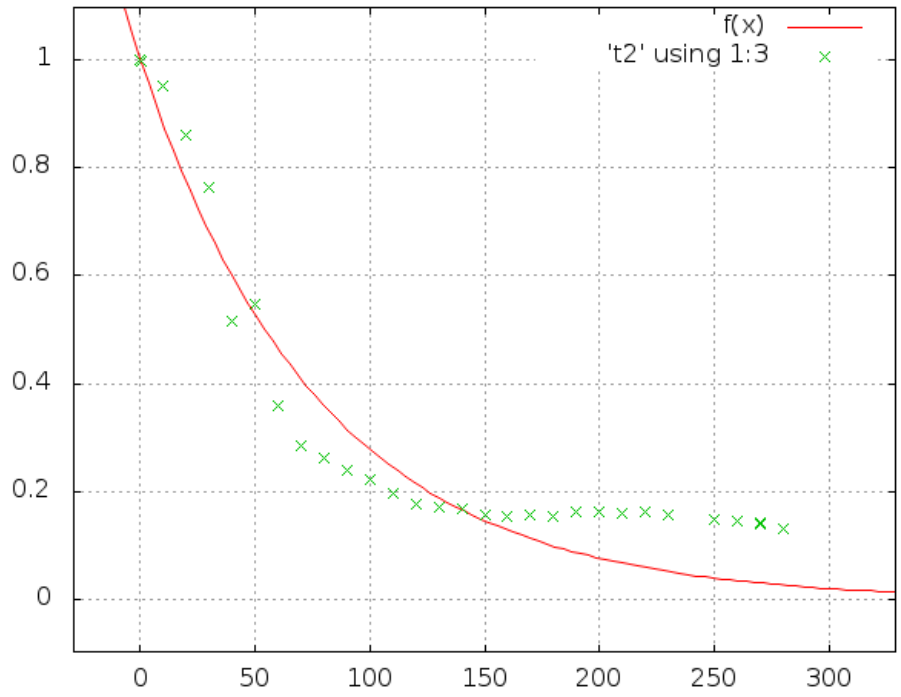

Figure 10: Intensity vs Time, for T_2, peak 1

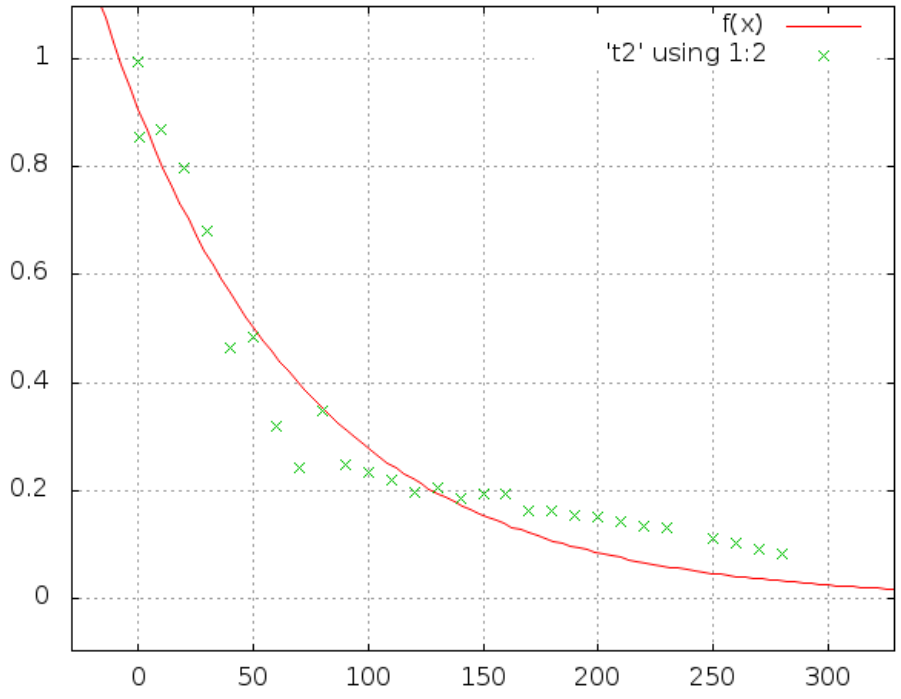

Figure 11: Intensity vs Time, for T_2, peak 2

COLOPHON

This document was typeset using the typographical look-and-feel `classicthesis` developed by André Miede, for LaTeX.
The style was inspired by Robert Bringhurst's seminal book on typography "*The Elements of Typographic Style*".

The latest version of this document is available online at:

https://github.com/toAtulArora/IISER_repo